V3 DockStar: overcome limitations of CombDock

Bioinformatics, 31(17), 2015, 2801–2807
doi: 10.1093/bioinformatics/btv270
Advance Access Publication Date: 25 April 2015
Original Paper

Structural bioinformatics

DockStar: a novel ILP-based integrative method for structural modeling of multimolecular protein complexes

Naama Amir*, Dan Cohen and Haim J. Wolfson*

Blavatnik School of Computer Science, Tel Aviv University, Tel Aviv, Israel

2 subtasks for generation of macromolecular complex structures:

(a) Identify the protein-protein **interaction graph** between the individual subunits.
This can be done e.g. based on data from MS and **chemical cross-linking**.

(b) Detect a globally consistent **pose** of the subunits, so that
- there are no steric clashes between them and
- the binding energy of the whole complex is optimized.

Chemical cross-linking

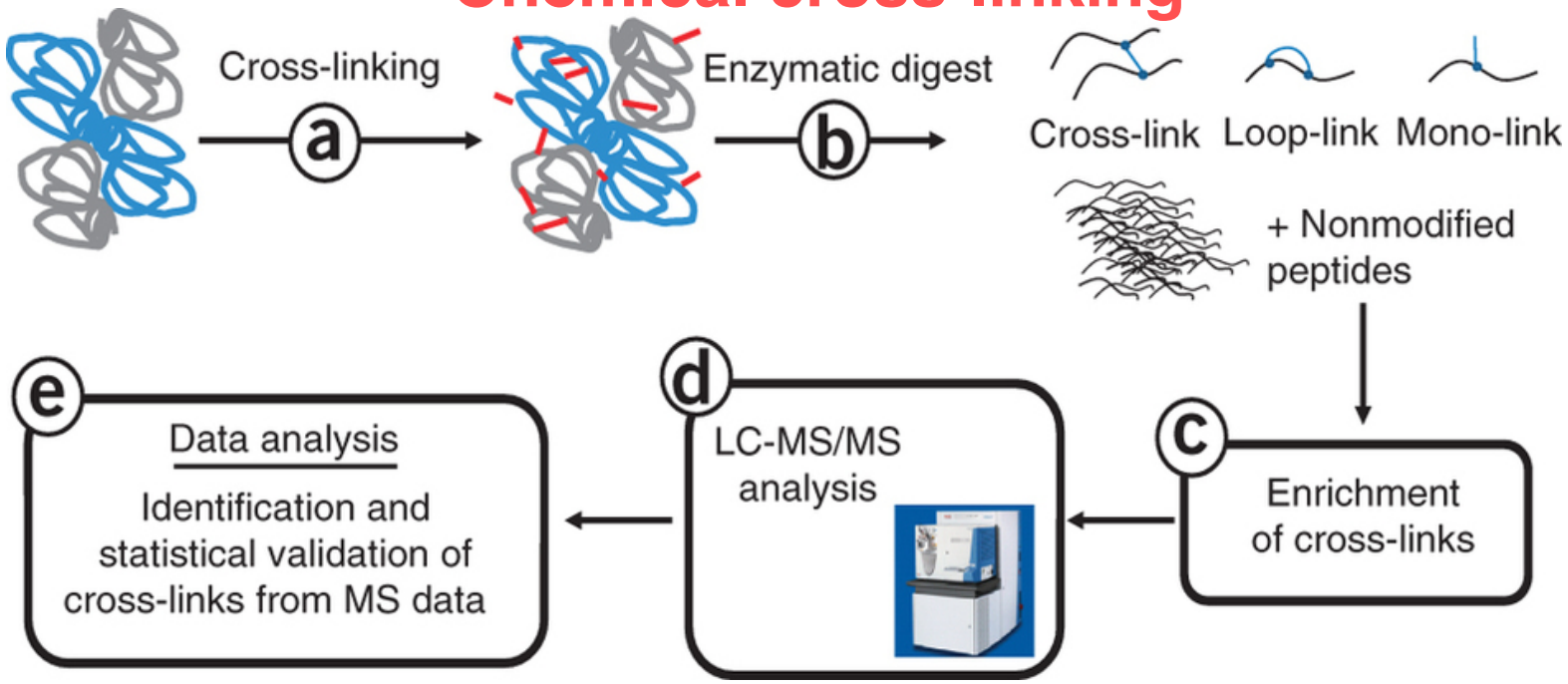

(**a**) Cross-linking reaction using a chemical cross-linking reagent. These molecules have a certain length, have two reactive groups at both ends of the molecule and may covalently bind either to cysteine or lysine residues of a single protein or of two proteins.

(**b**) enzymatic digestion of the proteins to peptides,

(**c**) enrichment of cross-linked peptides,

(**d**) analysis of cross-linked peptides by LC-MS/MS,

(**e**) data analysis.

Leitner et al. Nature Protocols 9, 120–137 (2014)

StarDock

- MS of intact protein complexes and their subcomplexes (→TAP-MS) can determine the **stoichiometry** of the complex subunits and deduce the **interaction graph** of the multimolecular complex.

- Chemical cross-linking combined with MS provides **distance constraints** between surface residues both on the same and on neighboring subunits.

This provides information both for the detection of the interaction graph as well as constraints on the relative spatial poses of neighboring subunits.

Amir et al., Bioinformatics 31, 2801 (2015)

Example: refining the 3D structure of S26 proteasome

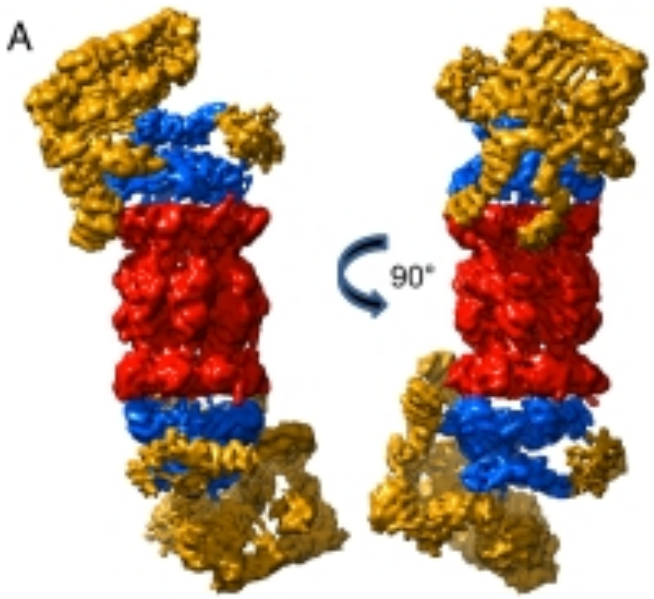

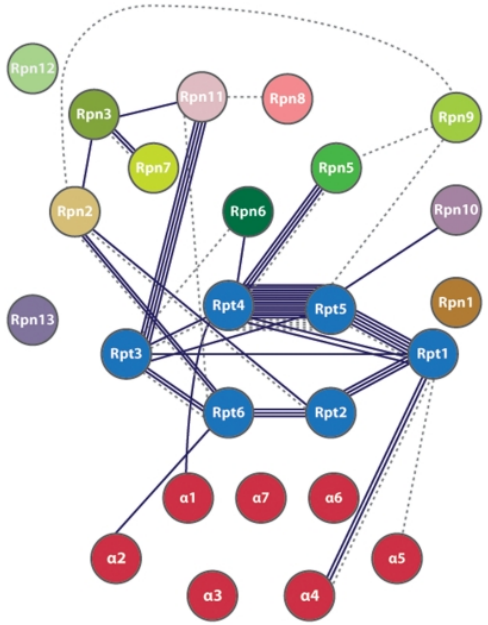

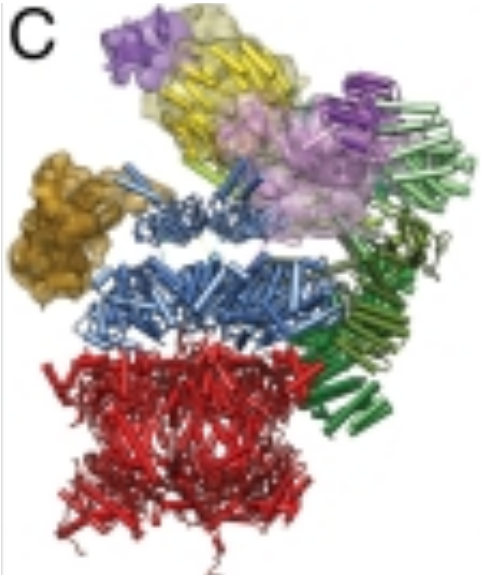

Low resolution

EM structure

Chemical cross-links for the *S. pombe* and *S. cerevisiae* 26S proteasomes.

55 (21) pairs of cross-linked lysines from the *S. pombe* (*S. cerevisiae*) 26S proteasome subunits.

Multiple edges between a pair of subunits indicate multiple cross-linked lysine pairs.

Atomistic structure generated

Lasker et al., PNAS (2012) 109: 1380

StarDock: Generate transformation sets

Assume that the **interaction graph** is **known** (task a).

Now we will generate for each subunit a set of candidate rigid transformations.

Select as **anchor subunit** the subunit having most neighbors in the multimolecular assembly interaction graph.

All other subunits which are known to interact with the anchor are then docked to it.

This requires a **star shaped spanning tree** topology of the interaction graph.

Pairwise docking is carried out by `PatchDock`, which optimizes shape complementarity, while satisfying maximal distance constraints between residues of neighboring subunits from cross-linking (details not important here).

The top 1000 `PatchDock` transformations are refined, rescored and re-ranked by the `FiberDock` tool → pairwise scores

Amir et al., Bioinformatics 31, 2801 (2015)

StarDock: Select best global solution

Let

- P_i $(0 \leq i < n)$ be **subunit** *i,*
- $T(P_i)$ be the set of **candidate transformations** for subunit P_i received from the previous stage.
- $T_{i,r}$ be a particular **transformation** *r* of subunit P_i .
- $S(T_{i,r}, T_{j,s})$ be the **pairwise interaction score** of subunits P_i and P_j transformed by $T_{i,r}$ and $T_{j,s}$, respectively (obtained by pairwise docking before).

The **globally optimal solution** Sol includes one transformation per subunit and maximizes the score(Sol) defined as:

$$\text{score}(\text{Sol}) = \sum_{T_{i,r}, T_{j,s} \in \text{Sol} \cap i \neq j} S(T_{i,r}, T_{j,s})$$

Amir et al., Bioinformatics 31, 2801 (2015)

DockStar: Select best global solution

This optimization task can be formulated as the following graph theoretic problem:

Let G = (V,E) be an undirected *n*-partite graph with a partition of the vertex set
$V = V_0 \cup \ldots \cup V_{n-1}$,
so that each transformation $T_{i,r} \in T(P_i)$ corresponds to a vertex $u_{i,r} \in V_i$.
(Each V_i contains all transformations r of subunit P_i as its vertices $u_{i,r}$).

Each pair of vertices is joined by an edge:

$$E = \{(u_{i,r}, v_{j,s}) | u_{i,r} \in V_i; v_{j,s} \in V_j; i \neq j\}$$

with the weight $w(u_{i,r}, v_{j,s}) = S(T_{i,r}, T_{j,s}) \qquad \forall (u_{i,r}, v_{j,s}) \in E$

The optimal solution is achieved by choosing one vertex per V_i
that maximizes the edge-weight of the induced sub-graph.

Amir et al., Bioinformatics 31, 2801 (2015)

Formulate Integer Linear Program (ILP)

This graph theoretic task can be formulated as an ILP. Define a variable $X_{i,r}$ for each vertex $u_{i,r} \in V$ and a variable $Y_{i,r,j,s}$ for each edge $e(u_{i,r}, v_{j,s}) \in E$ as follows

$$X_{i,r} = \begin{cases} 1 & \text{if } u_{i,r} \text{ is chosen} \\ 0 & \text{otherwise} \end{cases}$$

$$Y_{i,r,j,s} = \begin{cases} 1 & \text{if both } u_{i,r} \text{ and } v_{j,s} \text{ are chosen} \\ 0 & \text{otherwise} \end{cases}$$

The ILP **objective function** is

$$\text{Maximize} \qquad \text{score}(\text{Sol}) = \sum_{(u_{i,r}, v_{j,s}) \in E} w(u_{i,r}, v_{j,s}) Y_{i,r,j,s}$$

Subject to the constraints:

$$\sum_{u_{i,r} \in V_i} X_{i,r} = 1 \qquad \forall i, 0 \leq i < n$$

$$\sum_{u_{i,r} \in V_i} Y_{i,r,j,s} = X_{j,s} \qquad \forall j, s, i, \quad j \neq i$$

The objective function is exactly the edge-weight of the chosen sub-graph.
The first constraint ensures that exactly one transformation is chosen for each subunit.
The second constraint ensures that an edge is chosen if and only if both vertices that it connects are chosen as well.
The ILP step was solved by the CPLEX 12.5 package

Amir et al., Bioinformatics 31, 2801 (2015)

ILP formulation – alternative solutions

The ILP method outputs one single highest scoring global solution.

To retrieve additional high scoring solutions, the ILP step is applied iteratively to find a solution that maximizes the objective function and was not chosen before.

For this, a **linear constraint** is used (see paper by Amir et al.).

Amir et al., Bioinformatics 31, 2801 (2015)

ILP formulation – arbitrary complexes

Sofar we considered complexes having a **star shaped spanning tree**, where an **anchor** subunit, which interacts with all the other subunits, can be chosen. However, this is a special case.

Arbitrary complexes are divided into overlapping sub-complexes, each with a star shaped spanning tree, which are solved separately as above.

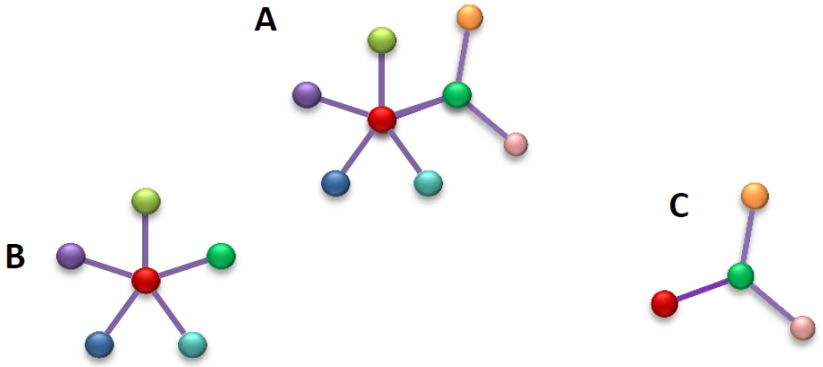

(A) A complex interaction graph that is **not star shaped**. Therefore, the complex is divided to 2 sub-complexes B and C and each sub-complex structure is solved separately. The transformation set for each subunit is generated by docking the subunit to the "anchor" subunit.

In (B) the anchor is represented by the red vertex and in (C) by the green. For each sub-complex a set of solutions is generated. Then, top solutions of these sub-complexes are integrated to create the 3D structure of the whole complex.

Amir et al., Bioinformatics 31, 2801 (2015)

DockStar applications

Table 1. Summary of the DockStar's results

Target complex	Bound/ unbound	Subunits number	Rank	Global Cα-RMSD[a]	Number of contacts[b]	Quality of predicted contacts[c]				Run time HH:MM
						high	medium	acceptable	lenient	
PP2A	Bound	3	1	0.68	2	2	0	0	0	00:35
	Unbound	3	1	6.9	2	0	0	0	2	00:43
Beef liver	Bound	4	1	0.85	3	3	0	0	0	02:51
Catalase	Unbound	4	1	2.7	3	0	3	0	0	03:53
RNA polII	Bound	11	1	7.9	10	4	3	2	0	04:53
	Unbound	11	3	4.8	10	0	3	4	1	04:56
Yeast exosome	Bound	10	1	5.1	9	6	1	0	0	10:34
	Unbound	10	12	6.0	9	1	1	1	1	11:22

[a]Global Cα-RMSD between the predicted and the native assemblies including only predictions with lenient to high quality.
[b]Number of contacts in the spanning tree of the complex interaction graph.
[c]Predicted interfaces in the target complex that are of lenient to high quality.

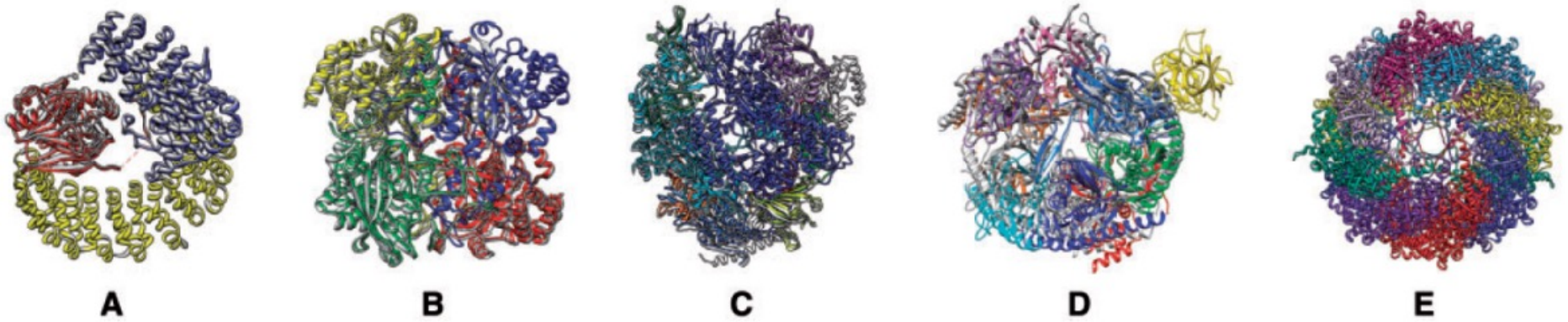

Fig. 1. The predicted models of the bound cases (coloured by chains) superimposed on the correct complex structures taken from the PDB (grey). (**A**) PP2A (A(yellow), B(blue), C(red)), (**B**) The Beef Liver Catalase [A(yellow), B(blue), C(red), D(green)], (**C**) RNA polymerase II [Rbp1(blue), Rbp2(cyan), Rbp3(light blue), Rbp5(purple), Rbp6(green), Rbp7(pink), Rbp8(yellow), Rbp9(dark green), Rbp10(orange), Rbp11(brown), Rbp12(red)], (**D**) The Yeast Exosome [Rrp45(blue), Rrp41(cyan), Rrp43(light blue), Rrp46(green), Rrp42(purple), Mtr3(pink), Rrp40(red), Rrp4(orange), Csl4(yellow), Dis3(dark green)]. (**E**) The predicted order of chains in the model of the TRiC/CCT Chaperonin: Z(red) Q(blue) H(yellow) E(light blue) B(pink) D(grey) A(green) G(purple)

Amir et al., Bioinformatics 31, 2801 (2015)

Mosaic-3D

Input:

(1) high-resolution 3D **structures** of a representative of each protein involved in forming the complex

(2) information on the **stoichiometry** of the complex.

(3) information on pairwise **interfaces** that provide the presumed binding modes in the complex.

Output:

3D-MOSAIC assembles the complex in an iterative tree-based greedy fashion.

Similar to CombDock, each node represents a monomer attached in a particular orientation.

Dietzen, Kalinina, Lengauer, Hildebrandt *et al.,*
Proteins 83, 1887-1899 (2015)

Mosaic-3D

The algorithm starts from a **seed monomer** with the largest number of interfaces.

In each iteration, new **child solutions** are generated by adding an additional monomer to each of the parent solutions retained from the previous iteration.

A new monomer of a particular protein type *p* can be attached to the complex *r* of a previous stage, if
i) the **number of occurrences** of *p* in the parent solution has not yet reached its maximum multiplicity,
ii) *r* has **unoccupied interfaces** for an interaction with *p*.
iii) The new monomer does not lead to severe **steric clashes** with other monomers already present in the parent solution.

The new child monomer is scored according to the number of interfaces it has with all ancestor monomers already present in the complex.

After each iteration: cluster solutions based on C_α-RMSD
Finally: optimize symmetry

Dietzen *et al,* Proteins 83, 1887-1899 (2015)

Workflow 3D-Mosaic

Assembly of homo-hexameric hemocyanin from *Panulirus interruptus* (1HCY.pdb).

In each iteration, new monomers can be attached to all previously retained solutions.

If a matching interface is found, the complex match score increases and the corresponding complex might be ranked further up in the list of solutions (green double-tilted arrows).

Solutions similar to better-ranked ones or yielding severe steric clashes are discarded.

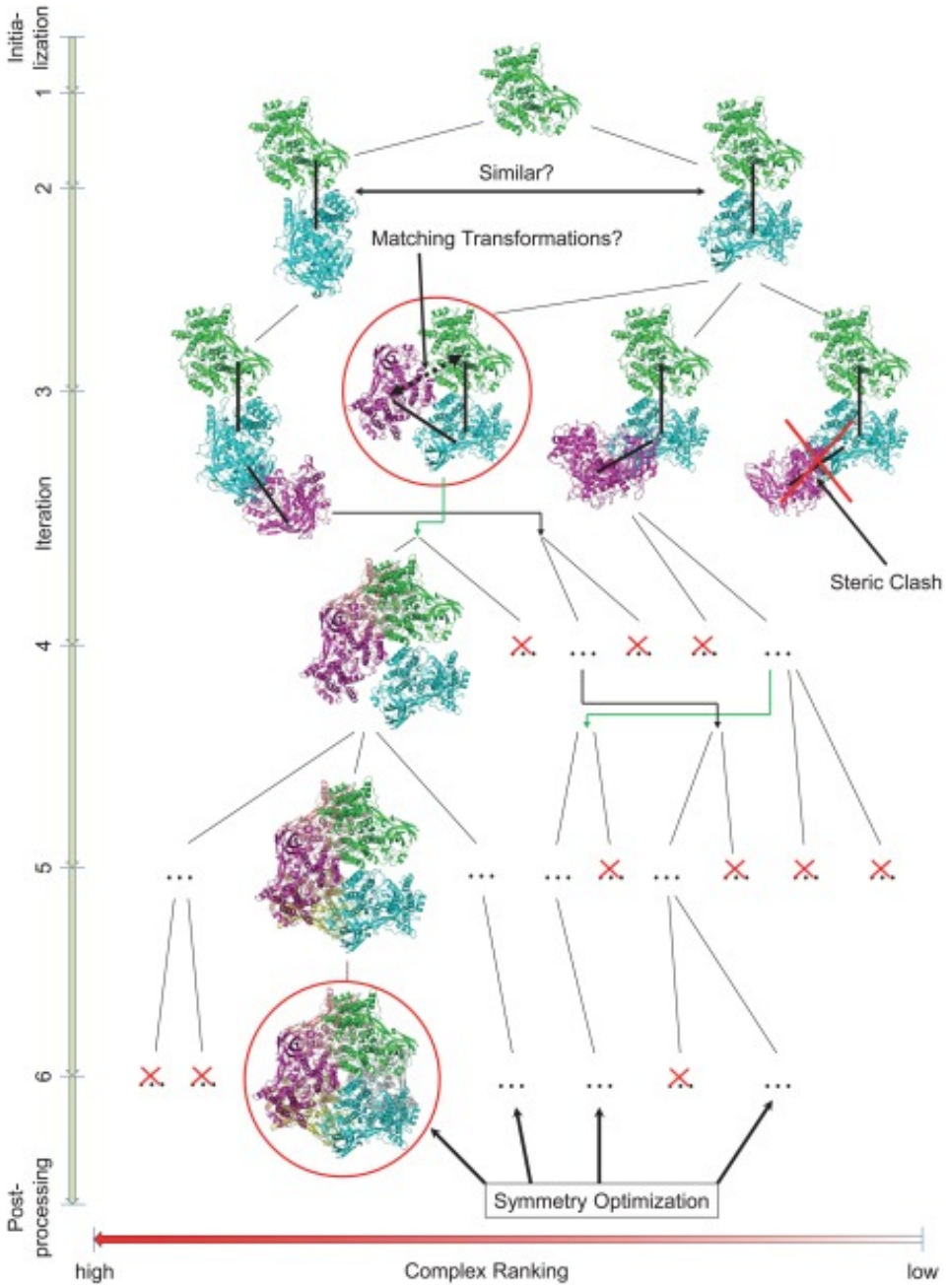

Dietzen et al, Proteins 83, 1887-1899 (2015)

Mosaic-3D

Examples of complexes and corresponding topology graphs for hard cases:
(**a**) ring-like topology of T4 lysozyme hexamer (3SBA),
(**b**) cage-like topology of pyruvate dehydrogenase E2 60-mer core complex (1B5S),
(**c**) inovirus coat protein filament (2C0W) composed of helical monomers,
(**d**) human cystatin C complex (1R4C) forming interchain β-sheets.
Different node colors correspond to different protein types, different edge colors to different binding modes.

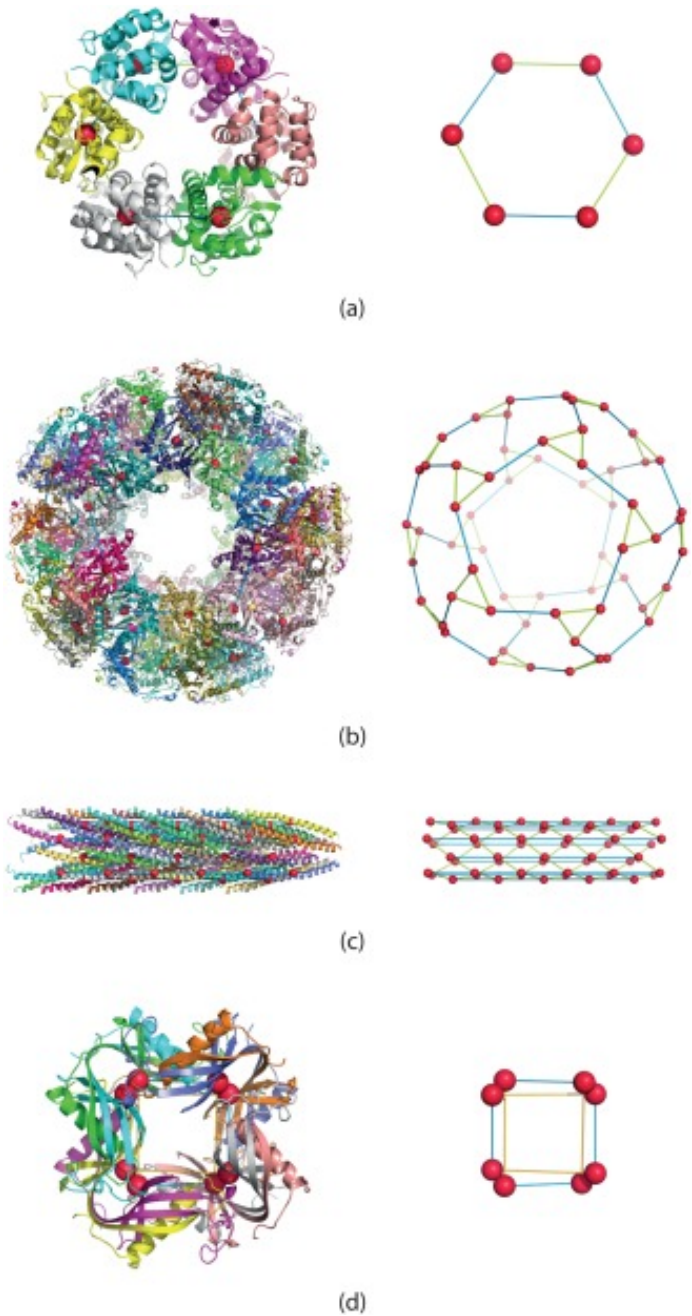

On a diverse benchmark set of 308 homo and heteromeric complexes containing 6 to 60 monomers, the mean fraction of correctly reconstructed benchmark complexes during crossvalidation was 78.1%.

Dietzen et al, Proteins 83, 1887-1899 (2015)

Summary

Our current atomistic understanding of how large macromolecular machines work is mainly based on results from protein crystallography. These discoveries were rewarded with several Nobel Prizes in Chemistry and Medicine.

Recent breakthrough: new detectors for EM that improve its resolution down to atomic resolution.

Ideal for structural characterization of large multi-protein complexes: combination of methods in structural biology:
- X-ray crystallography and NMR for high-resolution structures of single proteins and pieces of protein complexes
- (cryo) EM to determine high- to medium-resolution structures of entire protein complexes
- stained EM for still pictures at medium-resolution of cellular organells and
- (cryo) electron tomography for three-dimensional reconstructions of biological cells and for identification of the individual components.

Dietzen et al, Proteins 83, 1887-1899 (2015)

2.4 Fitting atomistic structures into EM maps

Atomistic structure of
a part of the complex

Coarse EM structure of
the whole complex

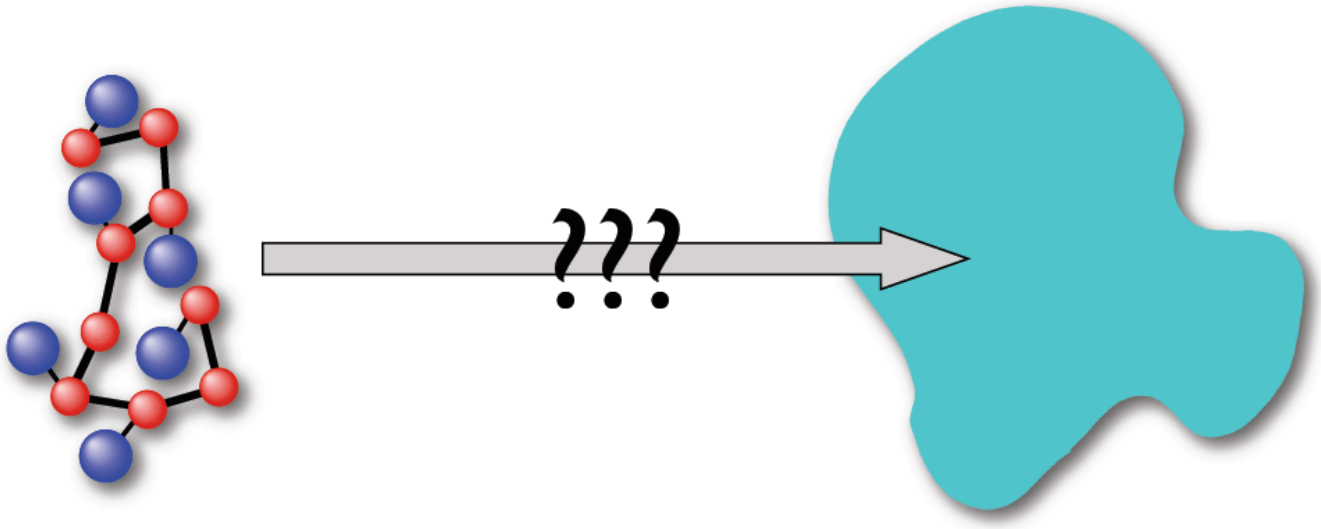

- same resolution for both structures
- exhaustive search with scoring
- choose best pose(s)

The procedure

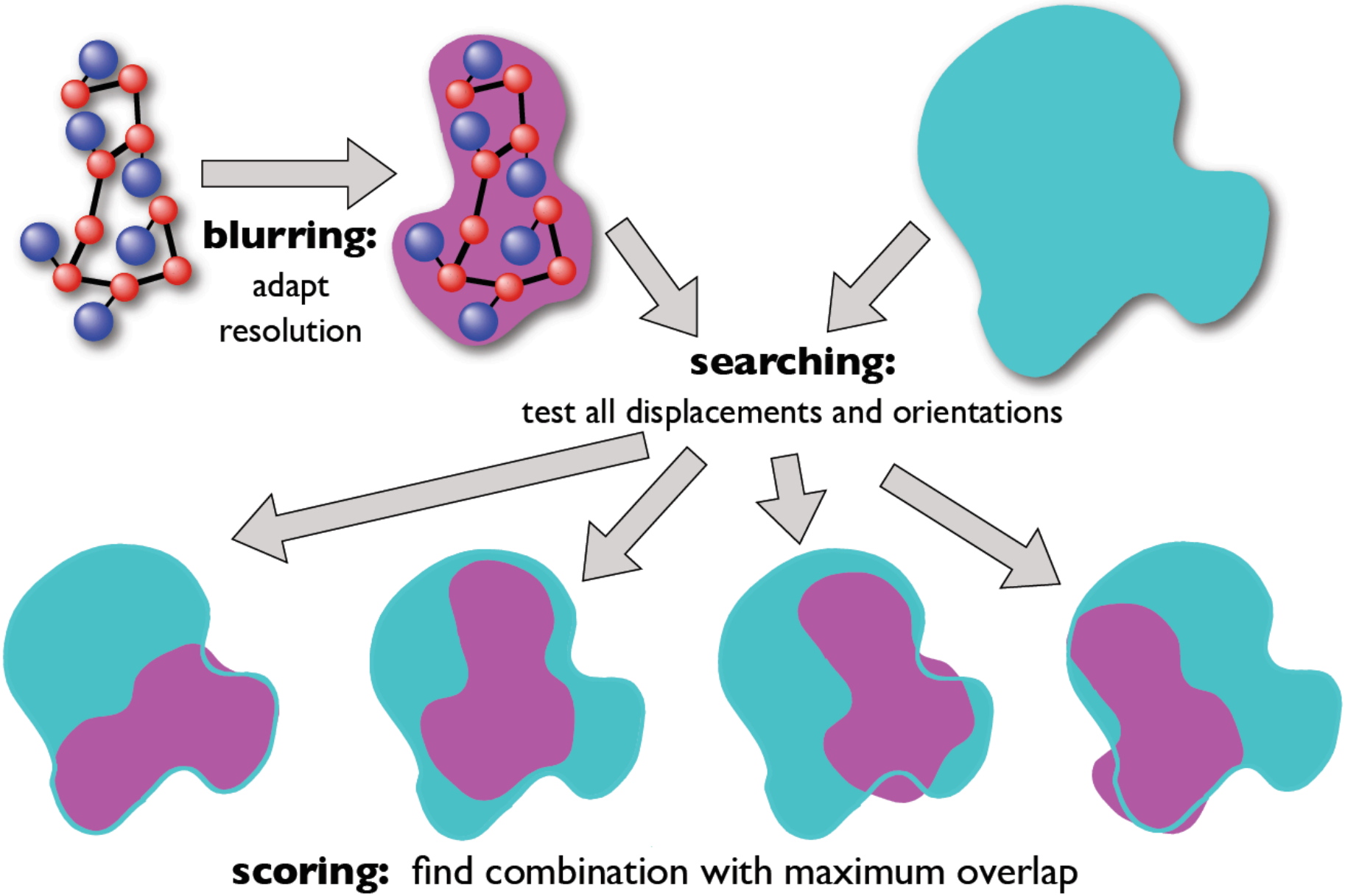

Step 1: blurring the picture

Mathematically:
convolution of (exact) atomistic structure f(x)
with experimental resolution g(x)

$$\tilde{f}(x) = (f \otimes g)(x) = \int dz\, f(z)\, g(x-z)$$

original data seen through the imaging apparatus

original signal

"kernel" => what is the image of a single point? (=delta signal)

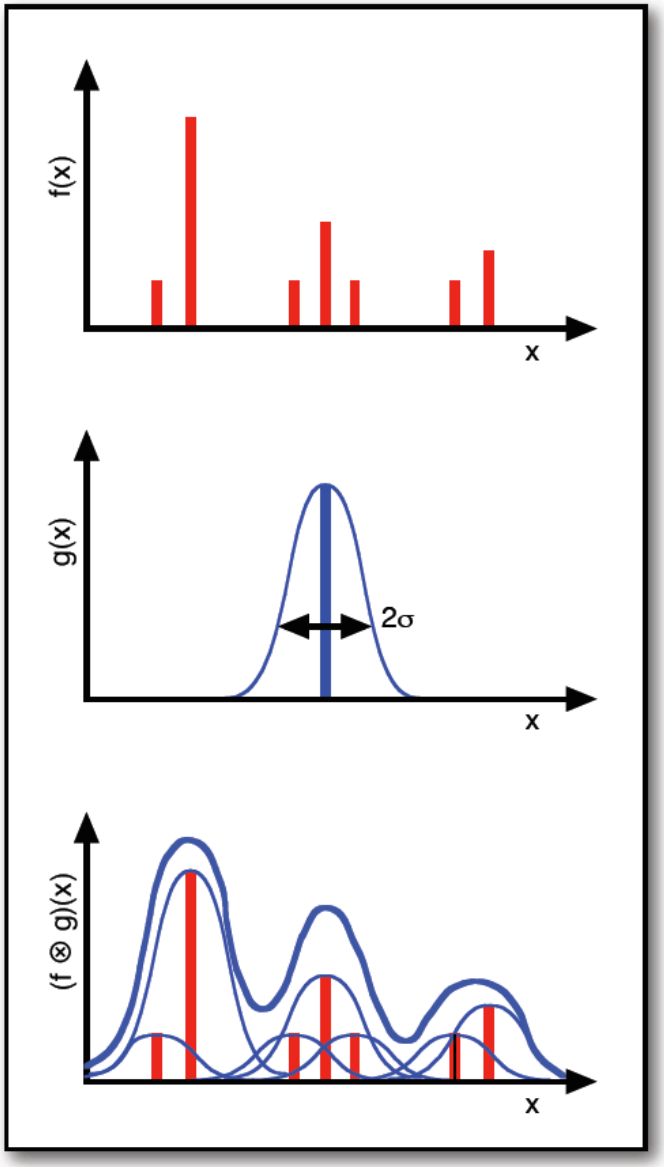

Often: blurring with gaussian

Put it on a grid

Discretize:

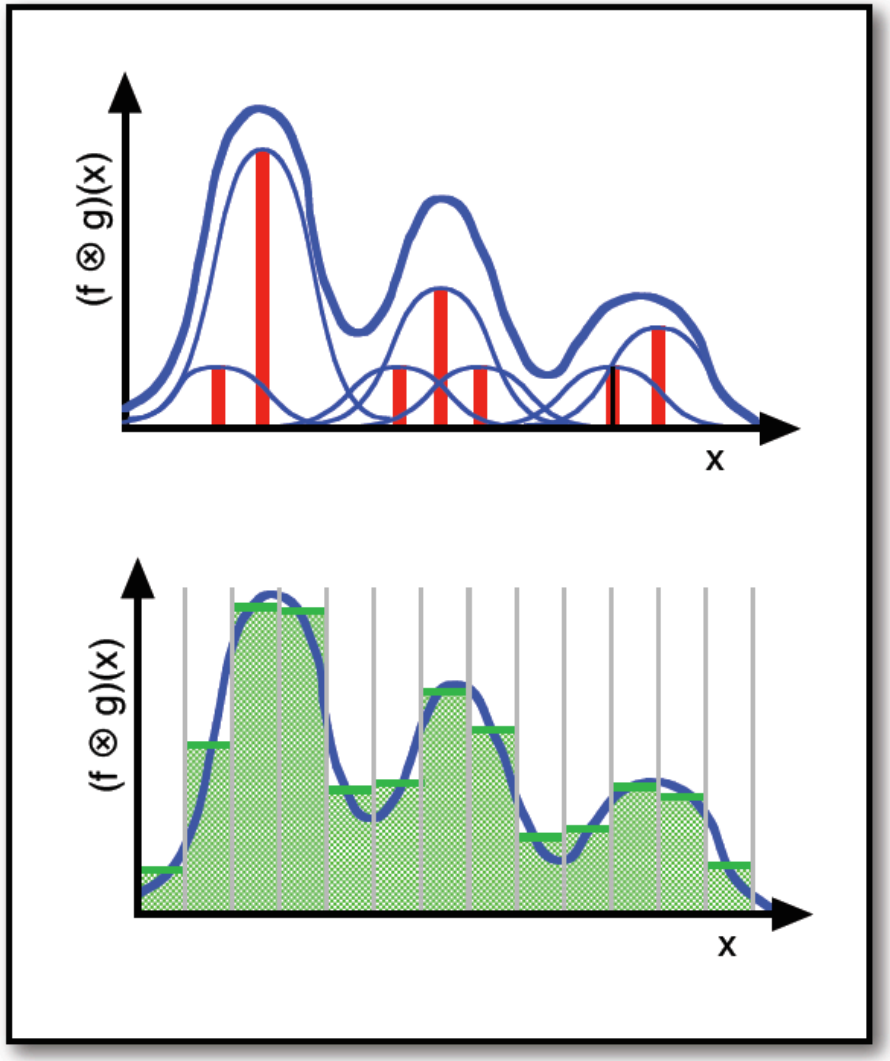

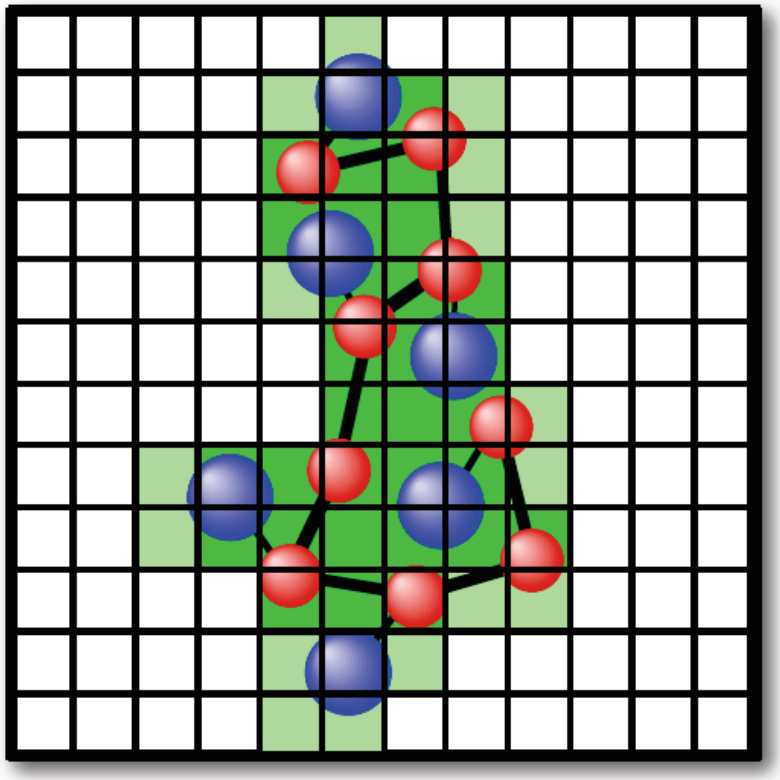

2.5 Fourier Transformation

Forward

$$F(k) = \int_{-\infty}^{\infty} dx\, e^{-ikx}\, f(x)$$

and inverse Fourier transform

$$f(x) = \frac{1}{2\pi} \int_{-\infty}^{\infty} dk\, e^{ikx}\, F(k)$$

with $$e^{ikx} = \cos(kx) + i \sin(kx)$$

=> convert between real and frequency (Fourier) space

short distances <=> high frequencies

long distances <=> low frequencies

Shift of the Argument

$$
\begin{aligned}
FT[f(x+\Delta x)] &= \int_{-\infty}^{\infty} dx\; e^{-ikx}\; f(x+\Delta x) \\
&= \int dy\; e^{-ik(y-\Delta x)}\; f(y) \\
&= e^{ik\,\Delta x} \int dy\; e^{-iky}\; f(y) \\
&= e^{ik\,\Delta x}\; FT[f(x)]
\end{aligned}
$$

Variable transformation:
$y = x + \Delta x$

change name of integration variable back from y to x

Convolution

$$\tilde{f}(x) = (f \otimes g)(x) = \int dz\, f(z)\, g(x-z)$$

Apply FT on both sides:

$$FT[\tilde{f}(x)] = FT[(f \otimes g)(x)] =$$

$$=$$

$$=$$

$$= FT[f(x)]\ FT[g(x)]$$

Integration in real space is replaced by simple multiplication in Fourier space.

But FTs need to be computed.

What is more efficient?

If the same width g(x) is used for multiple displaced datasets
=> do FT[g(x)] only once

Fourier on a Grid

On a finite grid: => maximum wavelength = length of grid
=> minimum wavelength = grid spacing
=> sum instead of integral

$$F_k = \sum_{j=0}^{N-1} e^{-2i\pi\, j\, k/N}\, f_j \qquad f_k = \frac{1}{N} \sum_{j=0}^{N-1} e^{+2i\pi\, j\, k/N}\, F_j$$

2.5.5 FFT by Danielson and Lanczos (1942)

Danielson and Lanczos showed that a discrete Fourier transform of length *N* can be rewritten as the sum of two discrete Fourier transforms, each of length *N*/2.

One of the two is formed from the even-numbered points of the original *N*, the other from the odd-numbered points.

F_k^e : *k*-th component of the Fourier transform of length *N*/2 formed from the even components of the original f_j 's

F_k^o : *k*-th component of the Fourier transform of length *N*/2 formed from the odd components of the original f_j *'s*

$$
\begin{aligned}
F_k &= \sum_{j=0}^{N-1} e^{-2\pi i k \frac{j}{N}} f_j \\
&= \sum_{j=0}^{\frac{N}{2}-1} e^{-2\pi i k \frac{2j}{N}} f_{2j} + \sum_{j=0}^{\frac{N}{2}-1} e^{-2\pi i k \frac{2j+1}{N}} f_{2j+1} \\
&= \sum_{j=0}^{\frac{N}{2}-1} e^{-2\pi i k \frac{j}{\frac{N}{2}}} f_{2j} + e^{-2\pi i k \frac{1}{N}} \sum_{j=0}^{\frac{N}{2}-1} e^{-2\pi i k \frac{j}{\frac{N}{2}}} f_{2j+1} \\
&= F_k^e + e^{-2\pi i k \frac{1}{N}} F_k^o
\end{aligned}
$$

FFT by Danielson and Lanczos (1942)

The wonderful property of the Danielson-Lanczos-Lemma is that it can be used recursively.

Having reduced the problem of computing F_k to that of computing F_k^e and F_k^o , we can do the same reduction of F_k^e to the problem of computing the transform of **its** $N/4$ even-numbered input data and $N/4$ odd-numbered data.

We can continue applying the DL-Lemma until we have subdivided the data all the way down to transforms of length 1.

What is the Fourier transform of length one? It is just the identity operation that copies its one input number into its one output slot.

For every pattern of $\log_2 N$ e‘s and o‘s, there is a one-point transform that is just one of the input numbers f_n

$$F_k^{eoeeoeo\ldots oee} = f_n \qquad \text{for some } n$$

FFT by Danielson and Lanczos (1942)

The next trick is to figure out which value of n corresponds to which pattern of e‘s and o‘s in $F_k^{eoeeoeo\ldots oee} = f_n$

Answer: reverse the pattern of e‘s and o‘s, then let e = 0 and o = 1,
and you will have, in binary the value of n.

This works because the successive subdividisions of the data into even and odd are tests of successive low-order (least significant) bits of n.

Thus, computing a FFT can be done efficiently in O(*N* log(*N*)) time.

Discretization and Convolution

For practical applications:
=> first put atomistic data onto the grid, then blur with FFT

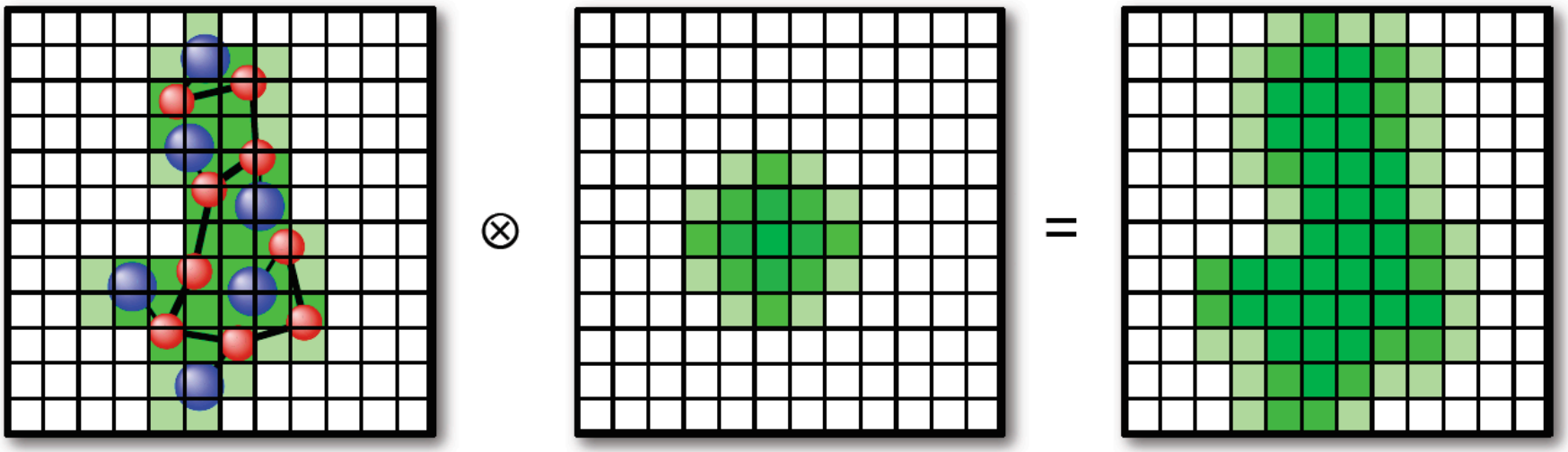

discretized hi-res data ⊗ blurring kernel = low-res image

Step 3: Scoring the Overlap

Most simple case:

- apply density threshold and count overlapping voxels
- displace images relative to each other, recount

=> find displacement with maximum overlap

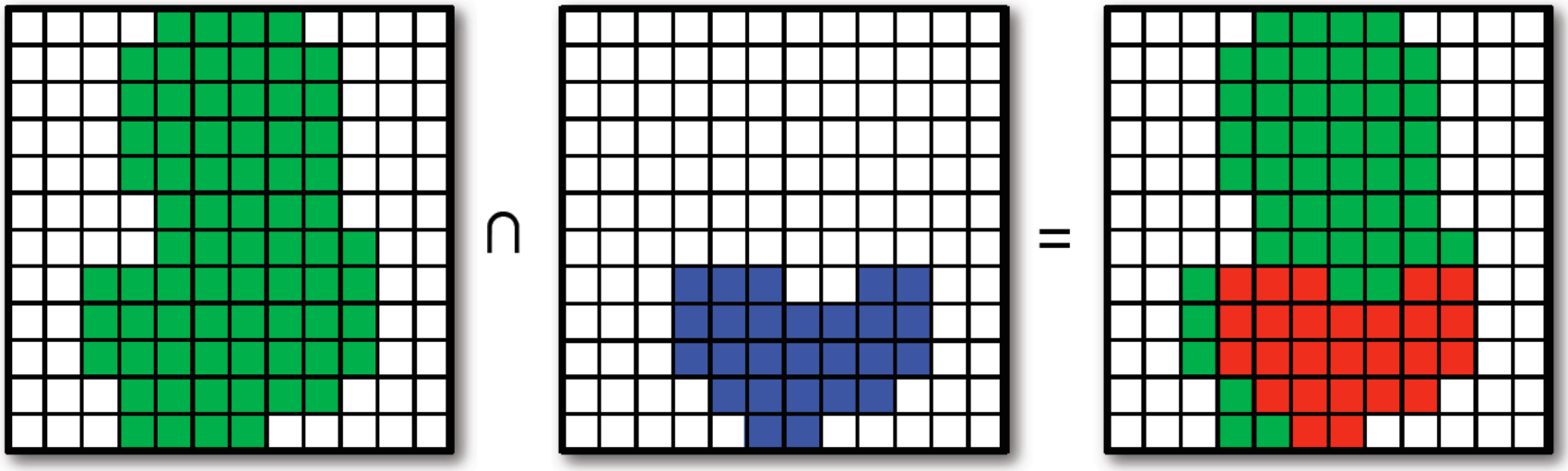

In matrix form with displacements x, y:

$$c(x,y) = \sum_{l=1}^{N} \sum_{m=1}^{N} a_{l,m}\, b_{l+x,m+y}$$

Cross Correlation

Generalization: maximize cross correlation of grided densities with respect to displacement (and orientation)

$$C_{x,y,z} = \sum_{l=1}^{N} \sum_{m=1}^{N} \sum_{n=1}^{N} a_{l,m,n} \times b_{l+x,m+y,n+z}$$

Note: maximize the cross-correlation <=> minimize the squared difference

On a grid with N^3 gridpoints => N^3 possible displacements
=> runtime $O(N^6)$

Further complication: the convolution

$$C_{x,y,z} = \sum_{l=1}^{N} \sum_{m=1}^{N} \sum_{n=1}^{N} a_{l,m,n} \times (g \otimes b_{l+x,m+y,n+z})$$

Correlation and Fourier

Apply Fourier transformation to both sides of

$$C_{x,y,z} = \sum_{l=1}^{N} \sum_{m=1}^{N} \sum_{n=1}^{N} a_{l,m,n} \times b_{l+x,m+y,n+z}$$

=> matrix multiplication

$$FT[C] = FT[A]^* \times FT[B]$$

Runtime of 3D FFT = $O(N^3 \log^3(N)) << N^6$

=> all possible displacements tested simultaneously

Note: FT[A] only calculated once initially

=> two FFTs per orientation

=> scan orientation via Euler angles

<== Step 2: exhaustive search

Include convolution

Maximize

$$C_{x,y,z} = \sum_{l=1}^{N} \sum_{m=1}^{N} \sum_{n=1}^{N} a_{l,m,n} \times (g \otimes b_{l+x,m+y,n+z})$$

In Fourier space:

Insert convolution $FT[f \otimes g] = FT[f] \times FT[g]$

Into correlation:

$$\begin{aligned} FT[C] &= FT[A]^* \times FT[G \otimes B] \\ &= FT[A]^* \times (FT[G] \times FT[B]) \\ &= (FT[A]^* \times FT[G]) \times FT[B] \end{aligned}$$

can be precomputed

2 FFTs + 1 matrix multiplication

2.7 Katchalski-Kazir algorithm

Proc. Natl. Acad. Sci. USA
Vol. 89, pp. 2195–2199, March 1992
Biophysics

Molecular surface recognition: Determination of geometric fit between proteins and their ligands by correlation techniques

(protein–protein interaction/surface complementarity/macromolecular complex prediction/molecular docking)

EPHRAIM KATCHALSKI-KATZIR[†‡], ISAAC SHARIV[§], MIRIAM EISENSTEIN[¶], ASHER A. FRIESEM[§], CLAUDE AFLALO[‖], AND ILYA A. VAKSER[†]

Departments of [†]Membrane Research and Biophysics, [§]Electronics, [¶]Structural Biology, and [‖]Biochemistry, Weizmann Institute of Science, Rehovot 76100, Israel

Contributed by Ephraim Katchalski-Katzir, October 24, 1991

Developed for protein-ligand docking
<=> same techniques applicable for docking "on the inside"

Discretization for docking

Next, to distinguish between the surface and the interior of each molecule, we retain the value of 1 for the grid points along a thin surface layer only and assign other values to the internal grid points. The resulting functions thus become

$$\bar{a}_{l,m,n} = \begin{cases} 1 & \text{on the surface of the molecule} \\ \rho & \text{inside the molecule} \\ 0 & \text{outside the molecule,} \end{cases} \quad [2a]$$

and

$$\bar{b}_{l,m,n} = \begin{cases} 1 & \text{on the surface of the molecule} \\ \delta & \text{inside the molecule} \\ 0 & \text{outside the molecule,} \end{cases} \quad [2b]$$

where the surface is defined here as a boundary layer of finite width between the inside and the outside of the molecule. The parameters ρ and δ describe the value of the points inside the molecules, and all points outside are set to zero. Two-

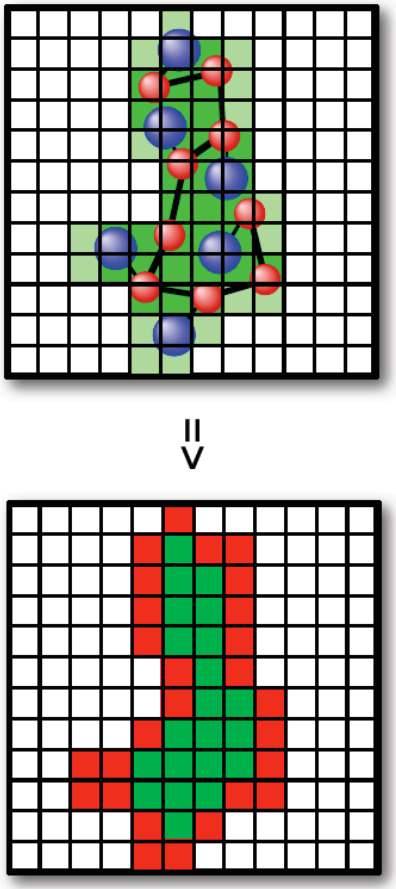

Typical values: $\rho = -15$, $\delta = 1$

=> penalty for overlap of volumes

Docking the hemoglobin dimer

2D cross sections at I = 46 (N = 90)

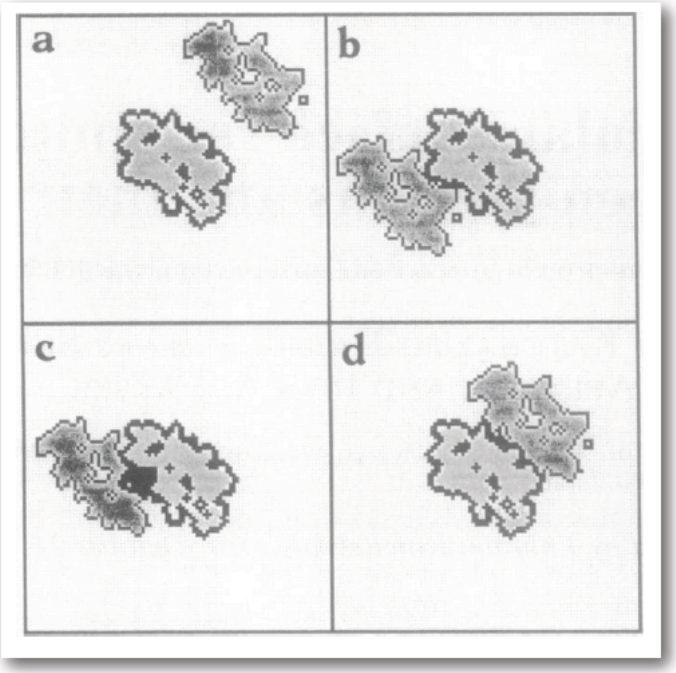

a) no contact
b) limited contact
c) overlap (black area)
d) good geometric match

Correlation at α = 0

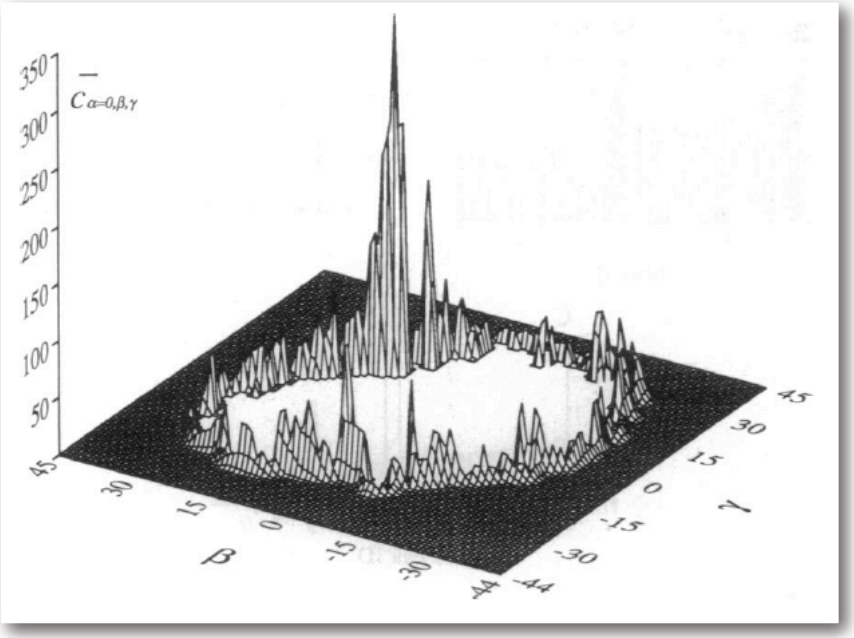

highest peak corresponds to native dimer arrangement

The algorithm

The entire procedure described above can be summarized by the following steps:
(*i*) derive $\bar{a}$ from atomic coordinates of molecule **a** (Eq. **2**),
(*ii*) $A^* = [\mathrm{DFT}(\bar{a})]^*$ (Eq. **4**),
(*iii*) derive $\bar{b}$ from atomic coordinates of molecule **b** (Eq. **2**),
(*iv*) $B = \mathrm{DFT}(\bar{b})$ (Eq. **4**),
(*v*) $C = A^* \cdot B$ (Eq. **5**),
(*vi*) $\bar{c} = \mathrm{IFT}(C)$ (Eq. **6**),
(*vii*) look for a sharp positive peak of $\bar{c}$,
(*viii*) rotate molecule **b** to a new orientation,
(*ix*) repeat steps *iii–viii* and end when the orientations scan is completed, and
(*x*) sort all of the peaks by their height.

Each high and sharp peak found by this procedure indicates geometric match and thus represents a potential complex. The relative position and orientation of the molecules within each such complex can readily be derived from the

Katchalski-Kazir et al. 1992

Algorithm has become a workhorse for docking and density fitting.

Problem I: limited contrast

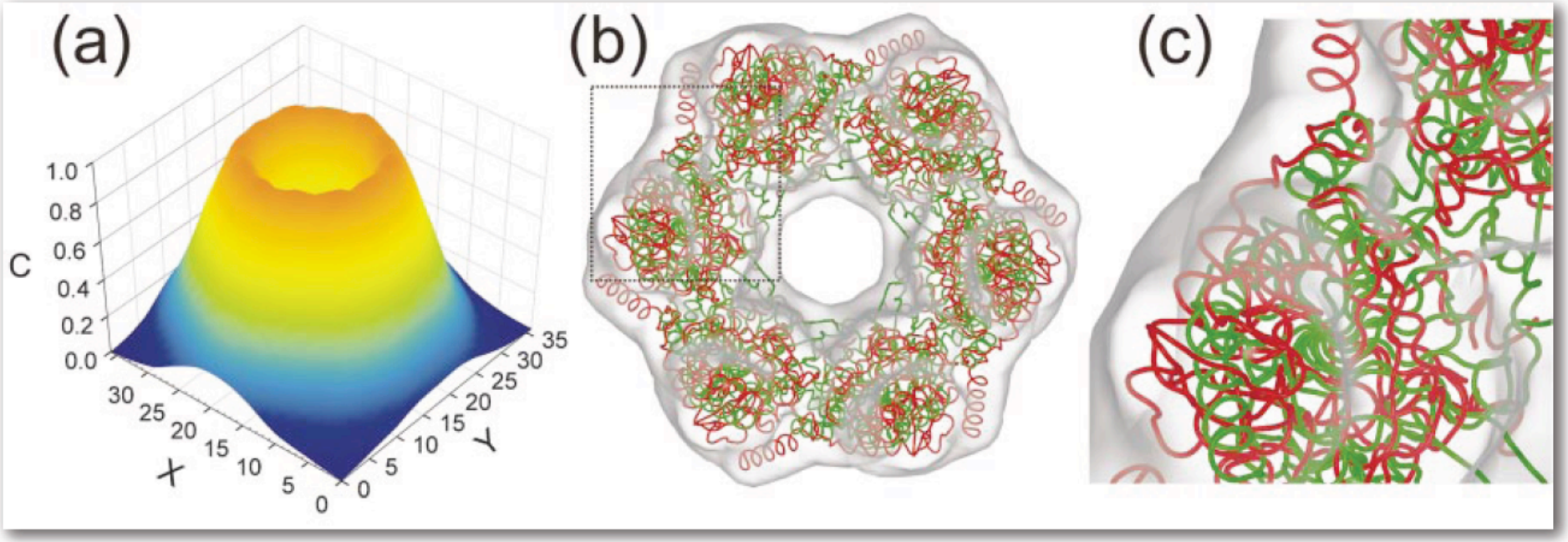

Docking of the RecA helicase monomer into simulated EM density of the hexamer at 15 Å resolution
(exhaustive 6D search with 5Å / 9° steps plus off-lattice optimization)
=> multiple fits with similar correlations

Chacón, Wriggers, *J. Mol. Biol.* **317** (2002) 375

2.6 Laplace filter

Evaluate $\nabla^2 = \frac{d^2}{dx^2} + \frac{d^2}{dy^2} + \frac{d^2}{dz^2}$

on a grid: $\nabla^2 a_{l,m,n} = -6a_{l,m,n} + a_{l+1,m,n} + a_{l-1,m,n} + a_{l,m+1,n} + a_{l,m-1,n} + a_{l,m,n+1} + a_{l,m,n-1}$

Correlation:

$$C_{x,y,z} = \sum_{l=1}^{N}\sum_{m=1}^{N}\sum_{n=1}^{N}(\nabla^2 \otimes a_{l,m,n}) \times (\nabla^2 \otimes g \otimes b_{l+x,m+y,n+z})$$

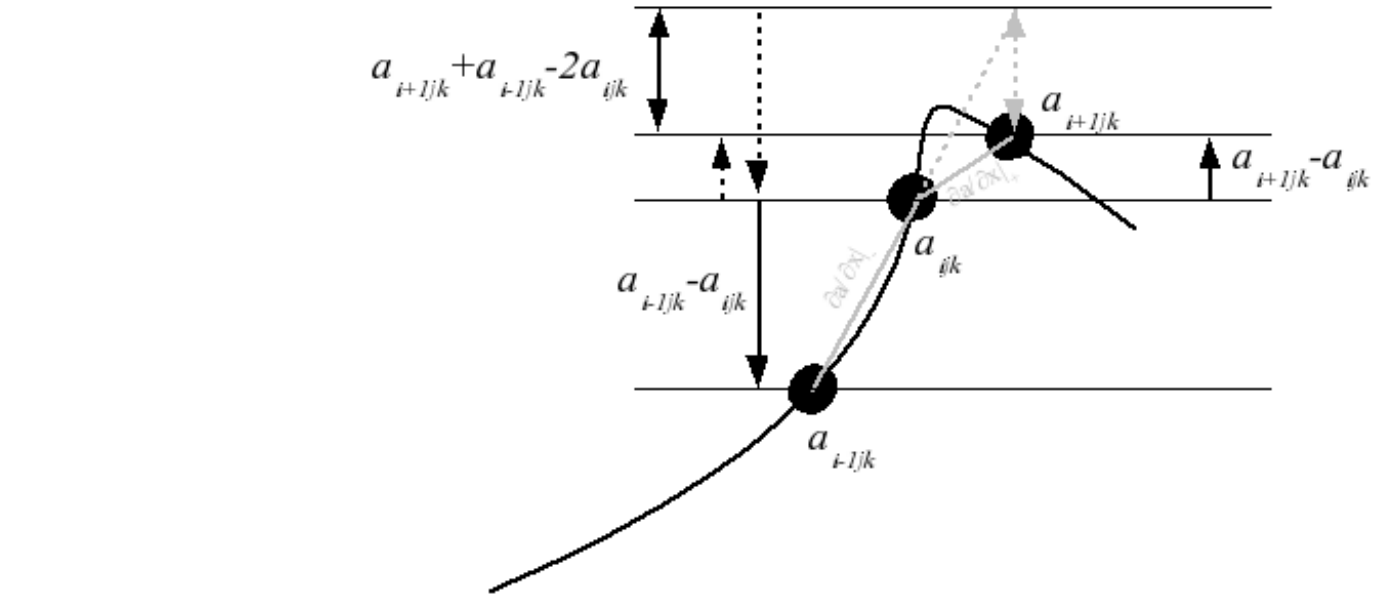

Enhanced contrast ➔ better fit

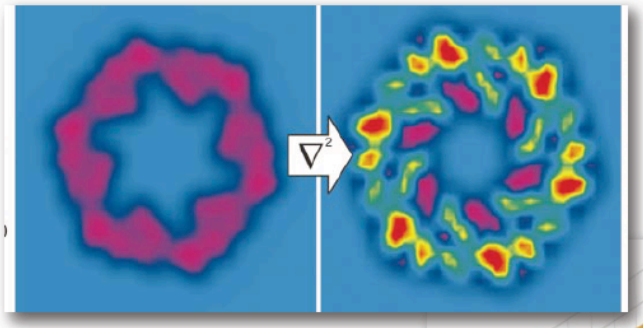

With the density alone:

With the Laplacian filter:

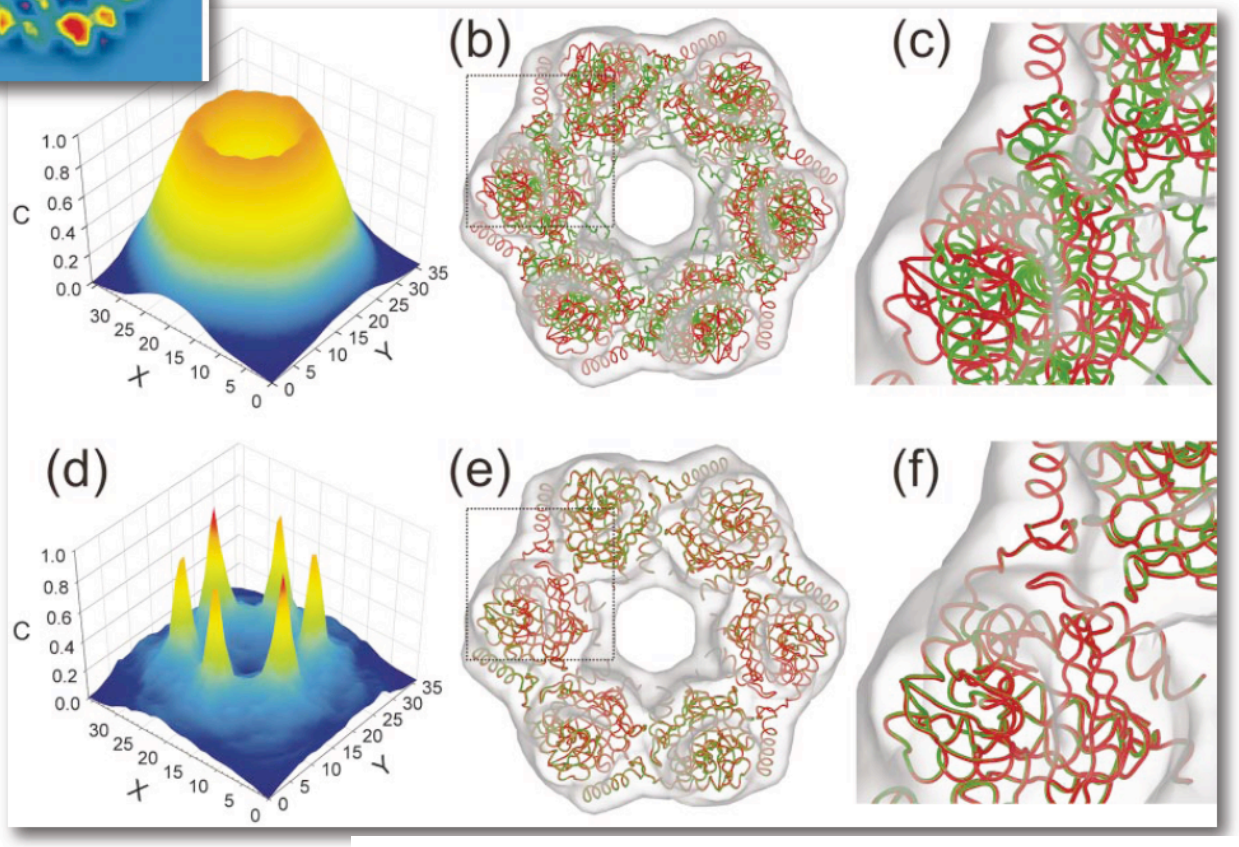

Chacón, Wriggers, *J. Mol. Biol.* **317** (2002) 375

The big picture

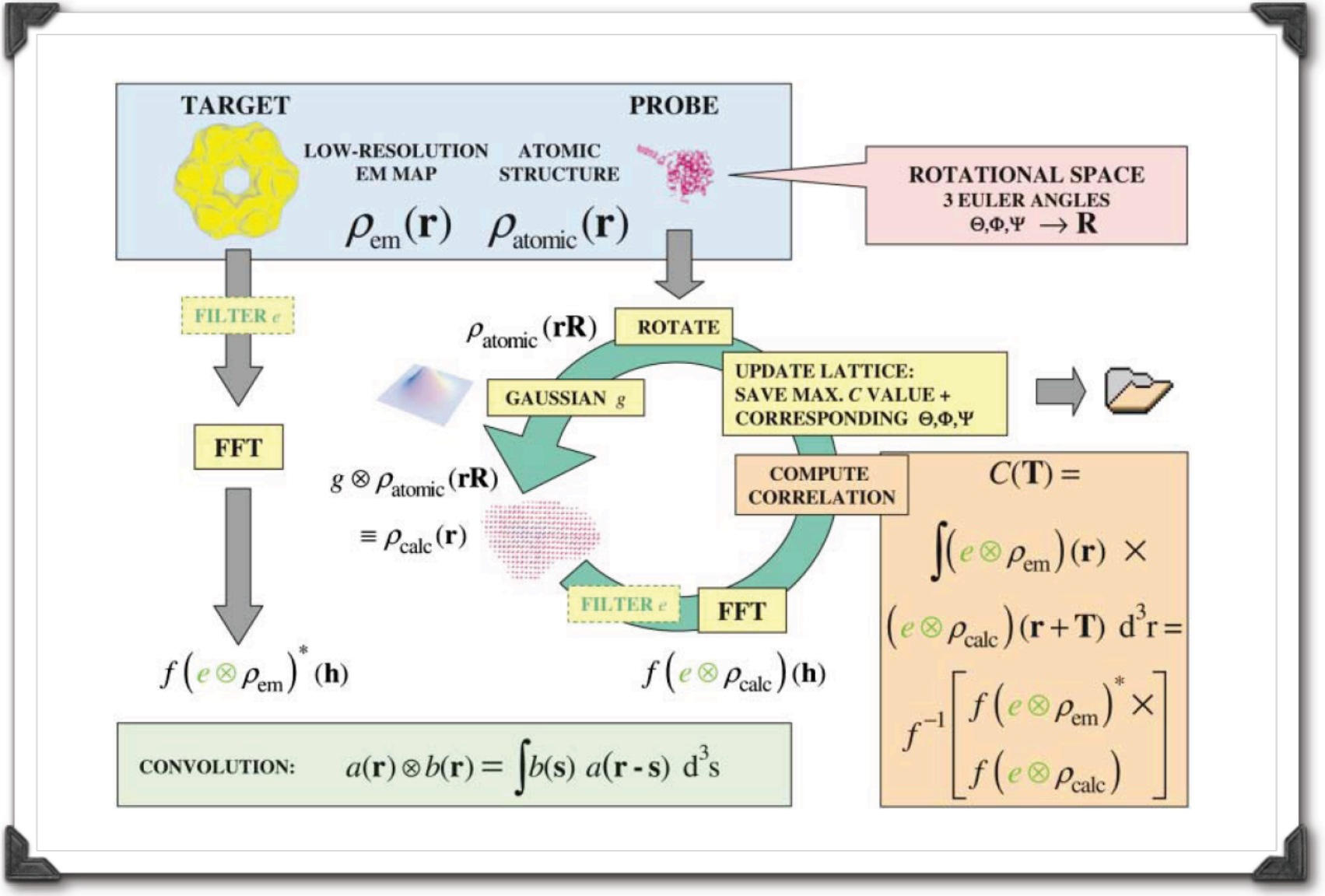

Wriggers, Chacón, *Structure* **9** (2001) 779

Problem 2: more efficient search

BIOINFORMATICS ORIGINAL PAPER

Vol. 23 no. 4 2007, pages 427–433
doi:10.1093/bioinformatics/btl625

Structural bioinformatics

ADP_EM: fast exhaustive multi-resolution docking for high-throughput coverage

José Ignacio Garzón, Julio Kovacs[1], Ruben Abagyan[1] and Pablo Chacón*

Centro de Investigaciones Biológicas, CSIC, Ramiro de Maeztu 9, 28040 Madrid, Spain and
[1]Department of Molecular Biology, The Scripps Research Institute La Jolla, CA 92037, USA

Received on September 28, 2006; revised on November 28, 2006; accepted on December 4, 2006
Advance Access publication December 6, 2006
Associate Editor: Alex Bateman

Observations:

- many displacements can be excluded a priori (FFT alg. calculates them all)
- FFT idea makes more sense for rotations (no simple limit on rotations)

Masked displacements

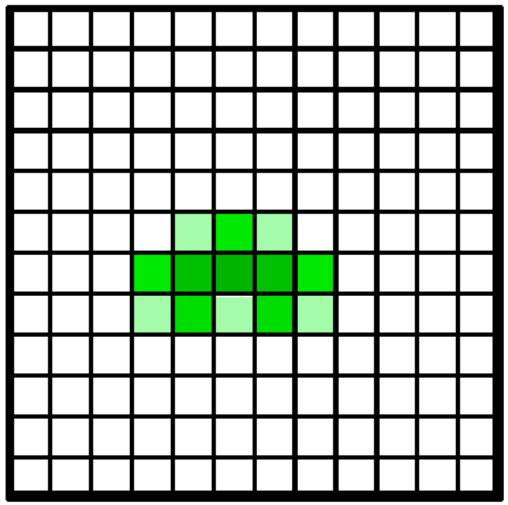

Probe

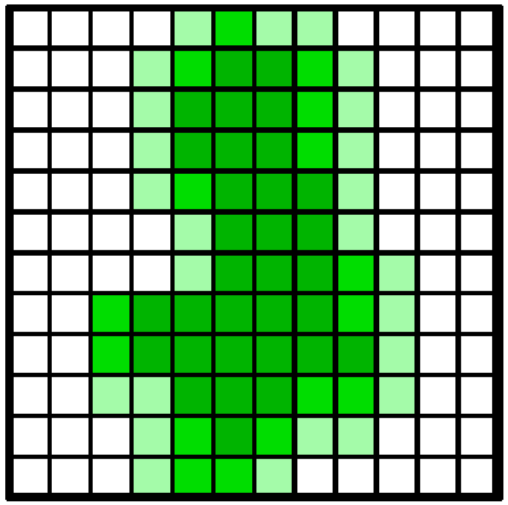

Target

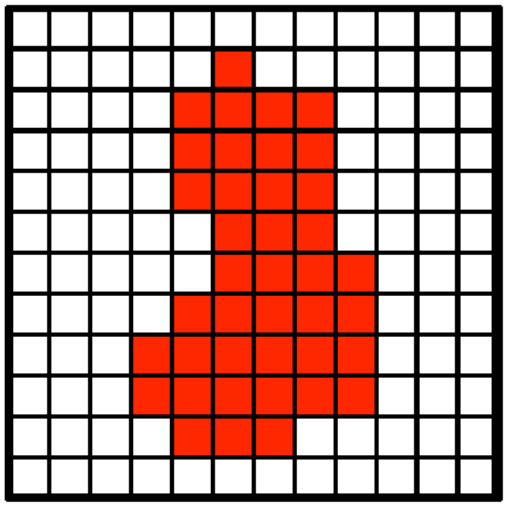

Mask =
potential hits

Search space for displacements =
(inside of the target molecule) – (extent of the probe)

Rotational search

Express densities in spherical harmonics on "onion shells"

$$\rho_{\text{low}}(r,\beta,\lambda) = \sum_{l=0}^{B-1} \sum_{m=-l}^{l} C_{lm}^{\text{low}}(r) Y_{lm}(\beta,\lambda) \qquad \rho_{\text{high}}(r,\beta,\lambda) = \sum_{l=0}^{B-1} \sum_{m=-l}^{l} C_{lm}^{\text{high}}(r) Y_{lm}(\beta,\lambda),$$

Y_{lm}	l = 0	l = 1	l = 2	l = 3
m = -3				$\sqrt{\frac{35}{64\pi}} \sin^3\vartheta\, e^{-3i\varphi}$
m = −2			$\sqrt{\frac{15}{32\pi}} \sin^2\vartheta\, e^{-2i\varphi}$	$\sqrt{\frac{105}{32\pi}} \sin^2\vartheta \cos\vartheta\, e^{-2i\varphi}$
m = −1		$\sqrt{\frac{3}{8\pi}} \sin\vartheta\, e^{-i\varphi}$	$\sqrt{\frac{15}{8\pi}} \sin\vartheta\, \cos\vartheta\, e^{-i\varphi}$	$\sqrt{\frac{21}{64\pi}} \sin\vartheta\, (5\cos^2\vartheta - 1)\, e^{-i\varphi}$
m = 0	$\sqrt{\frac{1}{4\pi}}$	$\sqrt{\frac{3}{4\pi}} \cos\vartheta$	$\sqrt{\frac{5}{16\pi}} (3\cos^2\vartheta - 1)$	$\sqrt{\frac{7}{16\pi}} (5\cos^3\vartheta - 3\cos\vartheta)$
m = 1		$-\sqrt{\frac{3}{8\pi}} \sin\vartheta\, e^{i\varphi}$	$-\sqrt{\frac{15}{8\pi}} \sin\vartheta\, \cos\vartheta\, e^{i\varphi}$	$-\sqrt{\frac{21}{64\pi}} \sin\vartheta\, (5\cos^2\vartheta - 1)\, e^{i\varphi}$
m = 2			$\sqrt{\frac{15}{32\pi}} \sin^2\vartheta\, e^{2i\varphi}$	$\sqrt{\frac{105}{32\pi}} \sin^2\vartheta \cos\vartheta\, e^{2i\varphi}$
m = 3				$-\sqrt{\frac{35}{64\pi}} \sin^3\vartheta\, e^{3i\varphi}$

Correlation for **all orientations** at a given displacement:

$$C(R) = FT^{-1}_{m,h,m'} \left[\sum_l d^l_{mh}\, d^l_{hm'} \int_0^\infty C_{lm}^{\text{low}}(r) \overline{C_{lm'}^{\text{high}}(r)} r^2 dr \right]$$

Known Fourier coefficients of spherical harmonics Y_{lm}.

Accuracy

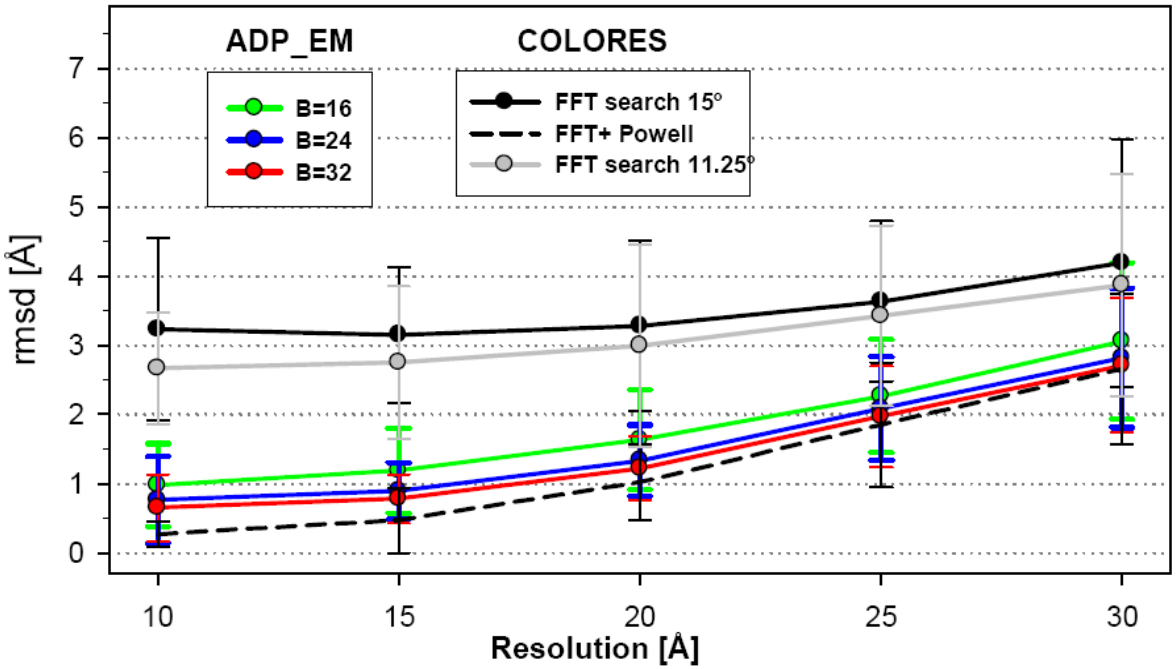

rmsd with respect to known atomistic structure of target.

Registration accuracy on simulated EM maps of 28 structures
for bandwidths (number of angular sampling points) of
B = 16, 24 32 (11°, 8°, ~ 6°)
compared to Wriggers' COLORES (situs package – Katchalski-Katzir algorithm + local Powell optimization)

Performance

Table 1. Timing results, in seconds, obtained with the benchmark described in Figure 1

	Sampling B/°	Resolution 10Å	15Å	20Å	25Å	30Å
ADP_EM	16/11°	28	31	35	34	38
	24/8°	100	108	119	118	123
	32/6°	226	220	225	216	221
FFT search	–/15°	1697	1926	2341	5028	6681
Powell minim	–/15°	375	918	1747	3739	6597

ADP_EM (Another Docking Platform for EM) is much faster

- only limited spatial region is scanned
- fast evaluation of the orientational correlation via FFT
- spherical harmonics allow for better rotational representation
  => higher accuracy

Some examples

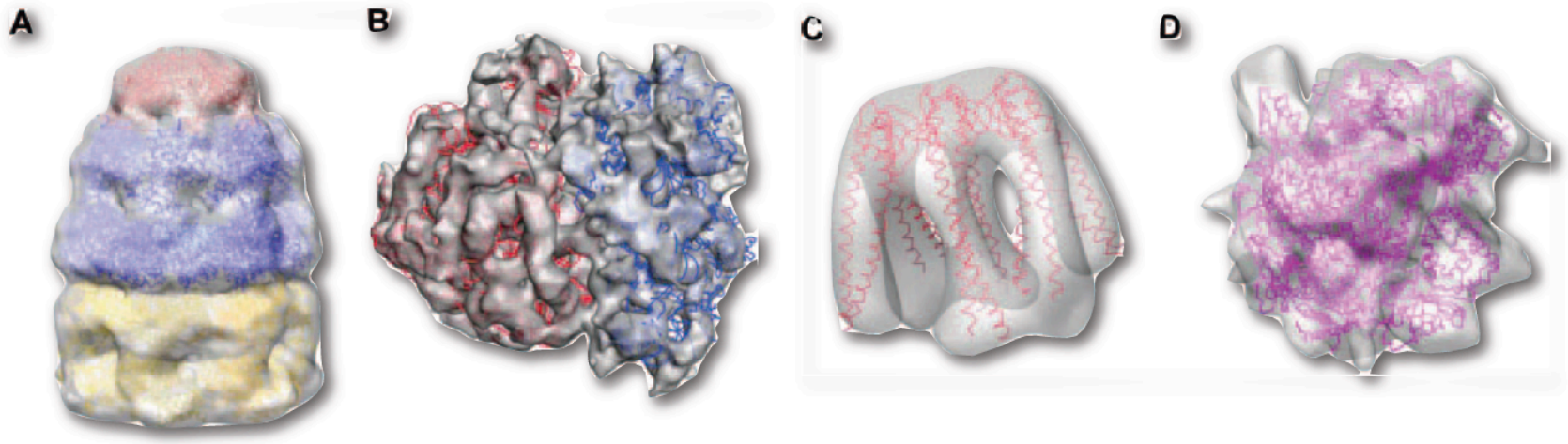

Fig. 2. Docking results with experimental EM data. (**A**) *E.coli* GroES-ADP7-GroEL-ATP7 from *E.coli* at 23.5 Å (EMD ID 1046, PDB: 1ml5); ADP and ATP GroEL subunits have been docked independently to reconstruct the cis and trans heptameric rings of the complex. For GroES the whole heptamer was used. (**B**) Docking of 30S and 50S subunits into *E.coli* ribosome map at 14 Å (EMD ID 1046, PDB: 1gix/1giy). Single-molecule docking of prefoldin (**C**) at 23 Å (Martin-Benito *et al.*, 2002), PDB: 1l6h, and of yeast RNA polymerase II (**D**) at 15 Å (Craighead *et al.*, 2002), PDB: 1fxk.

Summary

- StarDock
- Mosaic
- Density fitting of low-resolution structures into blurred density maps
    - analogy to FFT protein-protein docking
    - speed up by FFT-transforming the rotational angles